Journal of Energy Storage 19 (2018) 35–40

Contents lists available at ScienceDirect

Journal of Energy Storage

journal homepage: www.elsevier.com/locate/est

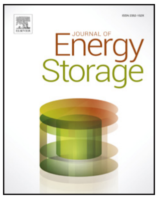

Excellent durable supercapacitor performance of hierarchical porous carbon spheres with macro hollow cores

Ming Zhou[a,b,*,1], Yun Lu[a,1], Huamai Chen[a], Xiaoxia Ju[a], Feng Xiang[a]

[a] *Institute of Technology, East China Jiao Tong University, Nanchang 330100, PR China*
[b] *Department of Chemistry, The University of Hong Kong, Pokfulam Rd, Hong Kong, China*

ARTICLE INFO

Keywords:
Carbon materials
Energy storage
Nano-materials
Porous structures

ABSTRACT

Hierarchical porous carbon spheres (HPCS) with 500 nm hollow cores and 100 nm shells have been prepared using hard template method. The synthesized HPCS has specific surface area up to 2489 $m^2\ g^{-1}$ and pore volume as high as 1.45 $cm^3\ g^{-1}$. The durable supercapacitor performance of HPCS is excellent with capacitance retention up to 99.7% after 10,000 charge/discharge tests at 10 $A\ g^{-1}$ from three-electrode testing and 97.1% after 10,000 cycles at 10 $mA\ cm^{-2}$ from two-electrode testing in 6 M KOH solution. HPCS also presents good supercapacitor performance with capacitance of 152 $F\ g^{-1}$ at scan rate of 2 $mV\ s^{-1}$ and keeps this capacitance of 123 $F\ g^{-1}$ at 100 $mV\ s^{-1}$. From the charge/discharge tests, HPCS displays capacitance up to 167 $F\ g^{-1}$ and 132 $F\ g^{-1}$ at current density of 0.2 $A\ g^{-1}$ and 20 $A\ g^{-1}$, respectively. From two-electrode testing, the capacitances of HPCS is 34.2 $mF\ cm^{-2}$ at 2 $mV\ s^{-1}$ and 37.4 $mF\ cm^{-2}$ at 0.5 $mA\ cm^{-2}$.

1. Introduction

Nowadays, many materials have been investigated as electrodes for supercapacitor applications [1]. Among them, porous carbons are promising due to their large surface area and low cost [2–13]. Activated carbons are the most widely utilized porous carbons for supercapacitors. However, micropores in activated carbons are not accessible at high rate, although the surface areas are high ($\geq 3000\ m^2\ g^{-1}$). This is not favourable for supercapacitors due to high ion transport resistance [14]. Ordered mesoporous carbons (OMCs) are also intensively studied [15–17]. Meanwhile, micron size of the particles increases the diffusion distance. Herein, carbon materials with macro-hollow structure are strongly recommended [18,19]. High-rate supercapacitor performance of a 3-D periodic porous carbon with macro hollow core has been reported by Li et al. [20].

In this article, monodisperse hierarchical porous carbon spheres with macro-hollow core have been synthesized. The electrochemical performance has been investigated. The results of the electrochemical characterizations will be discussed in details in following section. CMK-3 is utilized as a comparison as CMK-3 has mesopores at 3–5 nm without macro hollow structure.

2. Experimental

2.1. Preparation of hierarchical porous carbon spheres and CMK-3

In brief, silica hard templates were synthesized first. Then, carbon source (furfuryl alcohol, FA) and catalyst (oxalic acid, OA) were mixed together. After that, silica hard template was impregnated with precursors. The polymerization was conducted at 80 °C for 3 h and 160 °C for 3 h, followed by carbonization at 900 °C for 3 h in Ar. The silica hard template was removed in 10% hydrofluoric acid at room temperature. CMK-3 was synthesized following the published work [21] and details are given in supplementary information (SI).

2.2. Characterization

Transmission electron microscopy (TEM, Philips TECNAI 20 at 200 kV) and field emission scanning electron microscopy (SEM, Hitachi S-4800) were utilized to check the morphologies of the synthesized mesoporous carbon. Energy-dispersive X-ray spectroscopy (EDX) was operated on the SEM equipped with INCAx-sight EDX detectors (Oxford Instruments). Nitrogen sorption isotherms were obtained on a Micromeritics ASAP 2020 analyzer at 77 K. The surface area was calculated using Brunauer-Emmett-Teller (BET) method. The pore size distribution was derived from the desorption branch using Barrett-

---

[*] Corresponding author at: Institute of Technology, East China Jiao Tong University, Nanchang 330100, PR China.
E-mail address: zhoumingcn@outlook.com (M. Zhou).

[1] These authors contribute equally to this work.

https://doi.org/10.1016/j.est.2018.07.007
Received 8 June 2018; Received in revised form 8 July 2018; Accepted 8 July 2018
2352-152X/

Joyner-Halenda (BJH) method.

2.3. Electrochemical measurements

All the electrochemical experiments were performed on Solartron 1287. For a traditional three-electrode cell, Pt wire connected with Pt foil was used as counter electrode, Hg/HgO as reference electrode, and glassy carbon (GC) electrode (diameter: 6 mm) with active material deposition as working electrode, and 6 M KOH as electrolyte. For the preparation of working electrode, 20 mg HPCS was dispersed in the mixture of 1 mL DI water and 1 mL isopropanol, 2 mg PTFE power was used as binder. After that, 20 μL of the prepared ink was dripped onto the GC and dried at 60 °C for 4 h. The capacitance was calculated from both cyclic voltammetry (CVs) at scan rates from 2 to 100 mV s^{-1} and charge/discharge curves from 0.2 to 20 A g^{-1}. The applied voltage window is set between −0.9 and 0 V vs Hg/HgO. The cycling performance was tested through the repeating charge-discharge tests at 10 A g^{-1} for 10,000 cycles. Electrochemical impedance spectrum (EIS) was performed from 10^5 to 0.05 Hz with AC amplitude of 10 mV.

For the two-electrode testing system, 20 mg HPCS was dispersed in the mixture of 1 mL DI water and 1 mL isopropanol, 2 mg PTFE power was used as binder. After that, 0.25 mL of the prepared ink was dripped onto the round nickel foam disk with diameter of 2 cm and dried at 60 °C for 4 h. Then, two prepared electrodes were assembled to build up a symmetric two-electrode cell, using round filter paper with diameter of 2.5 cm as separator, which was soaked in 6 M KOH solution beforehand. Cyclic voltammetry (CVs) was performed at scan rates from 2 to 100 mV s^{-1} and charge/discharge curves from 0.5 to 20 mA cm^{-2}. The applied voltage window is set between −0.9 and 0.9 V. Cycling performance was also tested via repeating charge-discharge tests at 10 mA cm^{-2} for 10,000 cycles. EIS was performed from 10^5 to 0.05 Hz with AC amplitude of 10 mV.

3. Results and discussion

3.1. Morphologies, porosity, and components of HPCS

The morphology of HPCS is characterized by both SEM and TEM techniques (Fig. 1). The synthesized HPCS (Fig. 1a) are uniformly spherical with smooth surface, though several rough surfaces and broken structures observed. The overall diameter of HPCS is measured to be about 700 nm. Around 500 nm macro hollow core and 100 nm porous shell structure is verified by the TEM image (Fig. 1b), which is consistent to geometrical parameters observed from SEM. The porosity and surface area of HPCS is characterized using nitrogen sorption technique (Fig. 1c). As illustrated in the corresponding pore size distribution (inset of Fig. 1c), the pores in HPCS are mainly in the size regime of 2–4 nm and no information about micropores (< 2 nm) is provided because mesoporous model applied during testing. The BET specific surface area and pore volume of HPCS are 2489 $m^2 g^{-1}$ and 1.45 $cm^3 g^{-1}$, respectively. EDX is utilized to check the elemental composition of the synthesized HPCS (Fig. 1d). From the spectrum, there is one strong carbon peak and a relatively small oxygen peak, which is from the trapped small molecules (CO_2, CO) or the oxygen containing functional groups (>C═O, C−O−C) on the surface [22–24]. No any additional peak (Si) is found, indicating the total removal of silica hard template by HF solution [21]. The synthesized carbon materials are partially graphitized based on both Raman spectra (Fig. S1, supplementary information) and XRD pattern (Fig. S2). In the Raman spectrum, there is one strong D band together with a relatively weak G band, that is, the carbon materials are composed of both crystalline and amorphous components. This is further confirmed by the XRD pattern with low and wide diffraction peak.

3.2. Electrochemical performance of HPCS from three-electrode testing

Cyclic voltammetries (CV) are performed to evaluate the electrochemical performance of synthesized HPCS with scan rates from 2 to 100 mV s^{-1} (Fig. 2a). Typical rectangular and symmetrical CV curves are clearly observed even up to 100 mV s^{-1}, almost no any distortion presented, indicating identical electrical double layer capacitor (EDLC) behaviour with very low mass transport resistance [25]. The general functional group related peaks in the middle regime (−0.6 to −0.2 V vs Hg/HgO) are negligible in the CV curves of HPCS (Fig. 2a), which suggests the limited contribution from pseudocapacitance of functional groups [24]. The specific capacitances (Fig. 2b) are calculated from the CV curves at different scan rates derived from the following equation [20],

$$C = \frac{1}{2U \bullet \upsilon} \int |j| dE \tag{1}$$

where U is the applied voltage during CV scanning, υ is the scan rate and j is the current density. At the low rate (2 mV s^{-1}), HPCS gives the capacitance of 152.3 F g^{-1} while that of CMK-3 is only 125.3 F g^{-1}. This is derived from the higher surface area (2489 $m^2 g^{-1}$) and larger pore volume (1.45 $cm^3 g^{-1}$) of HPCS over those of CMK-3 (911 $m^2 g^{-1}$ and 0.78 $cm^3 g^{-1}$). The high surface area of HPCS is mainly contributed from the potential micropores (< 2 nm) and smaller mesopores (2–4 nm), which are only electrochemical accessible at very low rate [26,27]. On the other hand, this large surface area of HPCS is partially utilized as supercapacitor electrode during testing due to wetting issue. That is, the hydrophobic surface of HPCS cannot be fully wetted by the aqueous electrolyte. That is why only capacitance of 152.3 F g^{-1} is obtained from surface with area up to 2489 $m^2 g^{-1}$. The capacitances of HPCS and CMK-3 go down with the increased scanning rates and HPCS performs better with higher capacitances in the whole testing range. When the rate reaches 100 mV s^{-1}, HPCS maintains the capacitance at 123 F g^{-1} while the capacitance of CMK-3 is only 100 F g^{-1} at this rate. Under this condition, the small pores (potential micropores) in HPCS C are not accessible, that is, only outer mouth of the relatively larger pores (2– 4 nm) in HPCS can be utilized. The pores in CMK-3 mainly locate at around 3.6 nm (Fig. S3), nearly all the pores are able to be used at 100 mV s^{-1}. However, the electrochemical active area of HPCS is still comparable to that of CMK-3, though part surface area of HPCS is not accessible, as HPCS holds much larger surface area (2489 $m^2 g^{-1}$) over CMK-3 (911 $m^2 g^{-1}$). Furthermore, the diffusion distance of HPCS is narrowed down to 50 nm, where the macro hollow core serves as the active species reservoir (active species can be provided from both inner hollow core and outer surface across the 100 nm shell). Nevertheless, this distance of CMK-3 is still at micron level (Fig. S4) leading to much longer diffusion distance which greatly reduces high-rate performance of CMK-3 [18].

Galvanostatic charge/discharge tests are also conducted to characterize the electrochemical performance of HPCS (Fig. 2c). All the curves from 0.2 to 5.0 A g^{-1} display typical triangular and symmetrical characteristics, which again implies the ideal supercapacitor behaviour with excellent mass transport. High electrical conductivity of HPCS is also confirmed via the invisible *IR* drop on the discharge branches throughout the whole testing current ranges [28]. Specific capacitances of HPCS at different current densities from charge/discharge curves (Fig. 2d) are calculated based on the following equation [29],

$$C = \frac{I \Delta t}{mU} \tag{2}$$

where I is the current applied during tests, Δt is the time for the discharge side, m is mass of electrochemically active materials in gram, U is voltage window for tests in volts. HPCS presents better electrochemical performance at all current density range with 167 F g^{-1} at 0.2 A g^{-1}, 136 F g^{-1} at 10 A g^{-1} and maintaining the capacitance of 132 F g^{-1} at 20 A g^{-1} (79% capacitance retention compared with that